Beam-Target Double Spin Asymmetry A_{LT} in Charged Pion Production from Deep Inelastic Scattering on a Transversely Polarized ^{3}He Target at $1.4 < Q^2 < 2.7\,\mathrm{GeV}^2$

J. Huang,[1,*] K. Allada,[2] C. Dutta,[2] J. Katich,[3] X. Qian,[4,5] Y. Wang,[6] Y. Zhang,[7] K. Aniol,[8] J.R.M. Annand,[9] T. Averett,[3] F. Benmokhtar,[10] W. Bertozzi,[1] P.C. Bradshaw,[3] P. Bosted,[11] A. Camsonne,[11] M. Canan,[12] G.D. Cates,[13] C. Chen,[14] J.-P. Chen,[11] W. Chen,[4] K. Chirapatpimol,[13] E. Chudakov,[11] E. Cisbani,[15,16] J.C. Cornejo,[8] F. Cusanno,[15,16] M. M. Dalton,[13] W. Deconinck,[1] C.W. de Jager,[11,13] R. De Leo,[17] X. Deng,[13] A. Deur,[11] H. Ding,[13] P. A. M. Dolph,[13] D. Dutta,[18] L. El Fassi,[19] S. Frullani,[15,16] H. Gao,[4] F. Garibaldi,[15,16] D. Gaskell,[11] S. Gilad,[1] R. Gilman,[11,19] O. Glamazdin,[20] S. Golge,[12] L. Guo,[21] D. Hamilton,[9] O. Hansen,[11] D.W. Higinbotham,[11] T. Holmstrom,[22] M. Huang,[4] H. F. Ibrahim,[23] M. Iodice,[24] X. Jiang,[19,21] G. Jin,[13] M.K. Jones,[11] A. Kelleher,[3] W. Kim,[25] A. Kolarkar,[2] W. Korsch,[2] J.J. LeRose,[11] X. Li,[26] Y. Li,[26] R. Lindgren,[13] N. Liyanage,[13] E. Long,[27] H.-J. Lu,[28] D.J. Margaziotis,[8] P. Markowitz,[29] S. Marrone,[17] D. McNulty,[30] Z.-E. Meziani,[31] R. Michaels,[11] B. Moffit,[1,11] C. Muñoz Camacho,[32] S. Nanda,[11] A. Narayan,[18] V. Nelyubin,[13] B. Norum,[13] Y. Oh,[25] M. Osipenko,[33] D. Parno,[10] J. C. Peng,[6] S. K. Phillips,[34] M. Posik,[31] A. J. R. Puckett,[1,21] Y. Qiang,[4,11] A. Rakhman,[35] R. D. Ransome,[19] S. Riordan,[13] A. Saha,[11,†] B. Sawatzky,[31,11] E. Schulte,[19] A. Shahinyan,[36] M. H. Shabestari,[13] S. Širca,[37] S. Stepanyan,[25] R. Subedi,[13] V. Sulkosky,[1,11] L.-G. Tang,[14] A. Tobias,[13] G. M. Urciuoli,[15] I. Vilardi,[17] K. Wang,[13] B. Wojtsekhowski,[11] X. Yan,[28] H. Yao,[31] Y. Ye,[28] Z. Ye,[14] L. Yuan,[14] X. Zhan,[1] Y.-W. Zhang,[7] B. Zhao,[3] X. Zheng,[13] L. Zhu,[6,14] X. Zhu,[4] and X. Zong[4]

(The Jefferson Lab Hall A Collaboration)

[1] *Massachusetts Institute of Technology, Cambridge, MA 02139*
[2] *University of Kentucky, Lexington, KY 40506*
[3] *College of William and Mary, Williamsburg, VA 23187*
[4] *Duke University, Durham, NC 27708*
[5] *Kellogg Radiation Laboratory, California Institute of Technology, Pasadena, CA 91125*
[6] *University of Illinois at Urbana-Champaign, Urbana, IL 61801*
[7] *Lanzhou University, Lanzhou 730000, Gansu, People's Republic of China*
[8] *California State University, Los Angeles, Los Angeles, CA 90032*
[9] *University of Glasgow, Glasgow G12 8QQ, Scotland, United Kingdom*
[10] *Carnegie Mellon University, Pittsburgh, PA 15213*
[11] *Thomas Jefferson National Accelerator Facility, Newport News, VA 23606*
[12] *Old Dominion University, Norfolk, VA 23529*
[13] *University of Virginia, Charlottesville, VA 22904*
[14] *Hampton University, Hampton, VA 23187*
[15] *INFN, Sezione di Roma, I-00161 Rome, Italy*
[16] *Istituto Superiore di Sanità, I-00161 Rome, Italy*
[17] *INFN, Sezione di Bari and University of Bari, I-70126 Bari, Italy*
[18] *Mississippi State University, MS 39762*
[19] *Rutgers, The State University of New Jersey, Piscataway, NJ 08855*
[20] *Kharkov Institute of Physics and Technology, Kharkov 61108, Ukraine*
[21] *Los Alamos National Laboratory, Los Alamos, NM 87545*
[22] *Longwood University, Farmville, VA 23909*
[23] *Cairo University, Giza 12613, Egypt*
[24] *INFN, Sezione di Roma3, I-00146 Rome, Italy*
[25] *Kyungpook National University, Taegu 702-701, Republic of Korea*
[26] *China Institute of Atomic Energy, Beijing, People's Republic of China*
[27] *Kent State University, Kent, OH 44242*
[28] *University of Science and Technology of China, Hefei 230026, People's Republic of China*
[29] *Florida International University, Miami, FL 33199*
[30] *University of Massachusetts, Amherst, MA 01003*
[31] *Temple University, Philadelphia, PA 19122*
[32] *Université Blaise Pascal/IN2P3, F-63177 Aubière, France*
[33] *INFN, Sezione di Genova, I-16146 Genova, Italy*
[34] *University of New Hampshire, Durham, NH 03824*
[35] *Syracuse University, Syracuse, NY 13244*
[36] *Yerevan Physics Institute, Yerevan 375036, Armenia*
[37] *University of Ljubljana, SI-1000 Ljubljana, Slovenia*

(Dated: August 3, 2011)

We report the first measurement of the double-spin asymmetry A_{LT} for charged pion electroproduction in semi-inclusive deep inelastic electron scattering on a transversely polarized ^{3}He target. The kinematics focused on the valence quark region, $0.16 < x < 0.35$ with $1.4 < Q^2 < 2.7\,\mathrm{GeV}^2$. The corresponding neutron A_{LT} asymmetries were extracted from the measured ^{3}He asymmetries and proton/^{3}He cross section ratios using the effective polarization approximation. These new data probe the transverse momentum dependent parton distribution function g_{1T}^q and therefore provide access to quark spin-orbit correlations. Our results indicate a positive azimuthal asymmetry for π^- production on ^{3}He and the neutron, while our π^+ asymmetries are consistent with zero.

PACS numbers: 13.60.Le; 13.88.+e; 14.20.Dh; 24.85.+p

Understanding the spin structure of the nucleon in terms of parton spin and orbital angular momentum (OAM) remains a fundamental challenge in contemporary hadron physics. The transverse momentum dependent parton distribution functions (TMDs) [1, 2] describe the spin-correlated three-dimensional momentum structure of the nucleon's quark constituents. Of the eight leading-twist TMDs, five vanish after integration over transverse momentum, $\boldsymbol{p}_T$. Experimental information on these TMDs, including the transversal helicity g_{1T}^q, a T-even and chiral-even distribution that describes the longitudinal polarization of quarks in a transversely polarized nucleon [1, 3], is rather scarce. Because g_{1T}^q requires an interference between wave function components differing by one unit of quark OAM [4], the observation of a non-zero g_{1T}^q would provide direct evidence that quarks carry orbital angular momentum, constraining an important part of the nucleon spin sum rule [5].

In recent years, semi-inclusive deep-inelastic lepton-nucleon scattering (SIDIS) and the Drell-Yan process have been recognized as clean experimental probes for TMDs [6]. In the SIDIS process, $\ell(l) + N(P) \to \ell(l') + h(P_h) + X$, a lepton ($\ell$) scatters from a nucleon (N) and is detected in coincidence with a leading hadron (h) with particle four-momenta denoted by l, P, l' and P_h, respectively. All eight leading twist TMDs can be accessed using SIDIS [7]. In particular, the beam-helicity double spin asymmetry (DSA) A_{LT} in SIDIS reactions on a transversely polarized nucleon is given at leading twist by

$$A_{LT}\left(\phi_h,\phi_S\right) \equiv \frac{1}{|P_B S_T|}\frac{Y^+\left(\phi_h,\phi_S\right) - Y^-\left(\phi_h,\phi_S\right)}{Y^+\left(\phi_h,\phi_S\right) + Y^-\left(\phi_h,\phi_S\right)} \quad (1)$$
$$\approx A_{LT}^{\cos(\phi_h-\phi_S)}\cos\left(\phi_h-\phi_S\right),$$

where ϕ_h and ϕ_S are the azimuthal angles of the produced hadron and the target spin as defined in the Trento convention [8], P_B is the polarization of the lepton beam, S_T is the transverse polarization of the target, and $Y^{\pm}\left(\phi_h,\phi_S\right)$ is the normalized yield for beam helicity of ± 1. The partonic interpretation of the SIDIS cross section at the kinematic region of this experiment is supported by QCD factorization theory [9] and experimental data [10, 11]. At leading order (LO), the $A_{LT}^{\cos(\phi_h-\phi_S)}$ asymmetry is proportional to the convolution of g_{1T}^q and the unpolarized fragmentation function (FF) D_1 [3, 7].

In recent years significant progress in theory and phenomenology regarding g_{1T}^q and the related $A_{LT}^{\cos(\phi_h-\phi_S)}$ asymmetry has been achieved. In a light-cone constituent quark model [12], g_{1T}^q is explicitly decomposed into a dominant contribution from the interference of S- and P-waves and a minor ($< 20\%$) contribution from the interference of P- and D- waves in the quark wavefunctions. The $\boldsymbol{p}_T^2$-moment of g_{1T}^q can be calculated from the collinear g_1^q distribution function [13] using the Wandzura-Wilczek (WW)-type approximation [1, 3], which neglects the higher-twist contributions. In addition, the TMDs have recently been explored in lattice QCD, using a simplified definition of the TMDs with straight gauge links [14]. g_{1T}^q was among the first TMDs addressed with this method. g_{1T}^q has also been calculated in quark models as discussed in Refs. [15–22]. Common features of these models suggest that g_{1T}^u is positive and g_{1T}^d is negative. Both reach their maxima in the valence region at the few-percent level relative to the unpolarized distribution f_1^q. The simple relation $g_{1T}^q = -h_{1L}^{\perp q}$, where the $h_{1L}^{\perp q}$ TMD leads to the SIDIS A_{UL} asymmetry, has an essentially geometric origin and is supported by a large number of models [23]. Moreover, recent lattice QCD calculations indicate that the relation may indeed be approximately satisfied [14, 24]. In addition, the QCD parton model suggested approximate TMD relations, which link g_{1T}^q with the quark transversity distribution h_1^q and the pretzelosity distribution, $h_{1T}^{\perp q}$ [25]. $A_{LT}^{\cos(\phi_h-\phi_S)}$ has been predicted for the kinematics and reaction channels of this experiment using the WW-type approximations [26, 27], a light-cone constituent quark model [12, 16], a diquark spectator model [20] and a light-cone quark–diquark model [21].

The COMPASS collaboration previously reported preliminary results for $A_{LT}^{\cos(\phi_h-\phi_S)}$ in positive and negative charged hadron production using a muon beam scattered from transversely polarized deuterons [28] and protons [29]. The kinematics favored the sea quark region. Within the uncertainties, the preliminary results cannot differentiate between zero and various model predictions.

In this letter, we report new results from experiment E06-010 in Jefferson Lab Hall A, which measured the A_{LT} DSA and the target single spin asymmetries (target-SSA) [30] in SIDIS reactions on a transversely polarized ^{3}He target. The experiment used a longitudinally

polarized 5.9 GeV electron beam with an average current of 12 μA. Polarized electrons were excited from a superlattice GaAs photocathode by a circularly polarized laser [31] at the injector of the CEBAF accelerator. The laser polarization, and therefore the electron beam helicity, was flipped at 30 Hz using a Pockels cell. The average beam polarization was (76.8 ± 3.5) %, which was measured periodically by Møller polarimetry. Through an active feedback system [32], the beam charge asymmetry between the two helicity states was controlled to less than 150 ppm over a typical 20 minute period between target spin-flips and less than 10 ppm for the entire experiment. In addition to the fast helicity flip, roughly half of the data were accumulated with a half-wave plate inserted in the path of the laser at the source, providing a passive helicity reversal for an independent cross-check of the systematic uncertainty.

The ground state ^{3}He wavefunction is dominated by the S-state, in which the two proton spins cancel and the nuclear spin resides entirely on the single neutron [33]. Therefore, a polarized ^{3}He target is the optimal effective polarized neutron target. The target used in this measurement is polarized by spin-exchange optical pumping of a Rb-K mixture [34]. A significant improvement in target polarization compared to previous experiments was achieved using spectrally narrowed pumping lasers [35], which improved the absorption efficiency. The ^{3}He gas of ~10 atm pressure was contained in a 40-cm-long glass vessel, which provided an effective electron-polarized neutron luminosity of $10^{36}\,\mathrm{cm}^{-2}\mathrm{s}^{-1}$. The beam charge was divided equally among two target spin orientations transverse to the beamline, parallel and perpendicular to the central $\vec{l}$-$\vec{l}'$ scattering plane. Within each orientation, the spin direction of the ^{3}He was flipped every 20 minutes through adiabatic fast passage [36]. The average in-beam polarization was (55.4 ± 2.8)% and was measured during each spin flip using nuclear magnetic resonance, which in turn was calibrated regularly using electron paramagnetic resonance [37].

The scattered electron was detected in the BigBite spectrometer, which consists of a single dipole magnet for momentum analysis, three multi-wire drift chambers for tracking, a scintillator plane for time-of-flight measurement and a lead-glass calorimeter divided into pre-shower/shower sections for electron identification (ID) and triggering. Its angular acceptance was about 64 msr for a momentum range from 0.6 GeV to 2.5 GeV. The left High Resolution Spectrometer (HRS) [38] was used to detect hadrons in coincidence with the BigBite Spectrometer. Its detector package included two drift chambers for tracking, two scintillator planes for timing and triggering, a gas Cerenkov detector and a lead-glass calorimeter for electron ID. In addition, an aerogel Čerenkov detector and a ring imaging Čerenkov detector were used for hadron ID. The HRS central momentum was fixed at 2.35 GeV with a momentum acceptance of ±4.5% and an angular acceptance of ~6 msr.

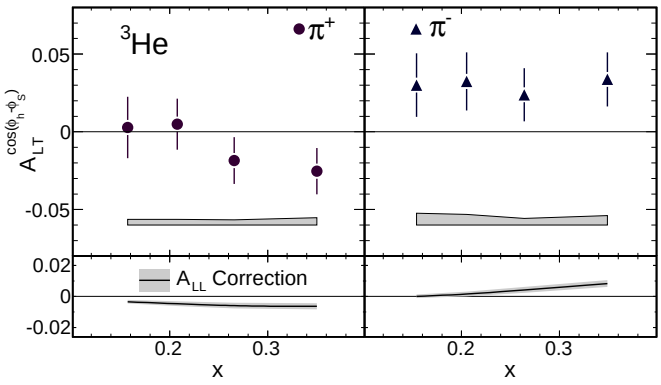

Figure 1. ^{3}He $A_{LT}^{\cos(\phi_h-\phi_S)}$ azimuthal asymmetry plotted against x for positive (top left) and negative (top right) charged pions. The A_{LL} correction (see text) that was applied and its uncertainty are shown in the bottom panels.

The SIDIS event sample was selected with particle identification and kinematic cuts, including the four momentum transfer squared $Q^2 > 1$ GeV^2, the virtual photon-nucleon invariant mass $W > 2.3$ GeV, and the mass of undetected final-state particles $W' > 1.6$ GeV. The kinematic coverage was in the valence quark region for values of the Bjorken scaling variable in $0.16 < x < 0.35$ at a scale of $1.4 < Q^2 < 2.7\,\mathrm{GeV}^2$. The range of measured hadron transverse momentum $P_{h\perp}$ was 0.24-0.44 GeV. The fraction z of the energy transfer carried by the observed hadron was confined by the HRS momentum acceptance to a small range about $z \sim$ 0.5-0.6. Events were divided into four x-bins with equivalent statistics. At high x, the azimuthal acceptance in $\phi_h - \phi_S$ was close to 2π, while at lower x, roughly half of the 2π range was covered, including the regions of maximal and minimal sensitivity to $A_{LT}^{\cos(\phi_h-\phi_S)}$ at $\cos(\phi_h - \phi_S) \sim \pm 1$ and zero, respectively. The central kinematics were presented in Ref. [30].

The beam-helicity DSA was formed from the measured yields as in Eq. (1). The azimuthal asymmetry in each x-bin was extracted directly using an azimuthally unbinned maximum likelihood estimator with corrections for the accumulated beam charge, the data acquisition livetime, and the beam and target polarizations. The result was confirmed by an independent binning-and-fitting procedure [30]. The sign of the asymmetry was cross-checked with that of the known asymmetry of $^3\vec{\mathrm{He}}(\vec{e}, e')$ elastic and quasi-elastic scattering on longitudinally and transversely polarized targets [39]. The small amount of unpolarized N_2 used in the target cell to reduce depolarization diluted the measured ^{3}He asymmetry, which was corrected for the nitrogen dilution defined as

$$f_{N_2} \equiv \frac{N_{N_2}\sigma_{N_2}}{N_{^3\mathrm{He}}\sigma_{^3\mathrm{He}} + N_{N_2}\sigma_{N_2}}, \qquad (2)$$

where N is the density and σ is the unpolarized SIDIS cross section. The ratio $\sigma_{^3\mathrm{He}}/\sigma_{\mathrm{N}_2}$ was measured periodically in dedicated runs on targets filled with known amounts of pure unpolarized ^{3}He and N_2, resulting $f_{\mathrm{N}_2} \sim 10\%$. A 5-20% longitudinal component of the target polarization with respect to the virtual photon direction introduced a small correction to $A_{LT}\left(\phi_h, \phi_S\right)$ from the DSA A_{LL}. A_{LL} and its uncertainty were calculated from the results of the DSSV 2008 global fit [13] combined with $P_{h\perp}$ dependence from a fit to recent proton data [40]. The A_{LL} uncertainty also includes a contribution from the longitudinal virtual-photon cross section, which was calculated using the SLAC-R1999 parametrization [41]. The A_{LT} results for ^{3}He and the A_{LL} correction applied to the data are shown in Fig. 1. Combining the data from all four x-bins, we have observed a positive asymmetry with 2.8 σ significance for π^- production on ^{3}He, while the π^+ asymmetries are consistent with zero.

The systematic uncertainties in our measurements due to acceptance, detector response drift and target density fluctuations were suppressed to a negligible level by the fast beam helicity reversal. With the addition of the frequent target spin reversal, the contributions from the beam-SSA A_{LU} and the target-SSA A_{UT} were canceled in the extraction of $A_{LT}^{\cos(\phi_h-\phi_S)}$. The dominant systematic effect for the lower x-bins was the contamination from photon induced charge-symmetric $e^{\pm}$ pair production, in which the e^- was detected in BigBite. The yield of (e^+, $\pi^{\pm}$) coincidences was measured by reversing the magnetic field of BigBite [30]. Since the measured asymmetry of the background was consistent with zero, the contamination was treated as a dilution. Bin centering ($|\delta A_{LT}/A_{LT}| \leq 14\%$) and radiative ($|\delta A_{LT}| \leq 0.1\%$) effects were estimated with an adapted SIMC Monte Carlo simulation [11] and POLRAD2 [42]. Other noticeable systematic uncertainties include the π^- contamination in the electron sample from BigBite ($|\delta A_{LT}| \leq 0.1\%$), the kaon contamination in the pion sample from the HRS ($|\delta A_{LT}| \leq 0.1\%$), and the beam and target polarimetry ($|\delta A_{LT}/A_{LT}| \leq 5\%$, each). Finally, uncertainties in the Cahn ($A_{UU}^{\cos\phi_h}$) and Boer-Mulders ($A_{UU}^{\cos 2\phi_h}$) effects on the unpolarized cross section [6] induce relative systematic uncertainties $|\delta A_{LT}/A_{LT}| \leq 10\%$ and 5%, respectively. The contamination in identified SIDIS events from decays of diffractively produced ρ mesons, estimated to range from 3-5% (5-10%) for π^+ (π^-) by PYTHIA6.4 [43], was not corrected, consistent with previous experimental analyses [30, 44, 45]. The uncertainties from neglecting the subleading-twist $\cos\phi_S$ and $\cos\left(2\phi_h - \phi_S\right)$ modulations associated with A_{LT} in the extraction procedure were not included due to a lack of experimental information and a general assumption that such effects are suppressed.

The neutron asymmetry was extracted from the ^{3}He asymmetry using the effective polarization approximation, given by

$$A_{LT}^n = \frac{1}{\left(1-f_p\right)P_n}\left(A_{LT}^{^3\mathrm{He}} - f_p A_{LT}^p P_p\right), \qquad (3)$$

where the proton dilution factor $f_p \equiv 2\sigma_p/\sigma_{^3\mathrm{He}}$ was measured with unpolarized ^{3}He and hydrogen gas targets in identical kinematics, including the uncertainties from spin-independent final state interactions (FSI) [30]. The effective neutron and proton polarizations in ^{3}He are given by $P_n = 0.86^{+0.036}_{-0.02}$ and $P_p = -0.028^{+0.009}_{-0.004}$ [46], respectively. Due to the small proton polarization and a scarcity of existing data, no A_{LT}^p correction was applied to our results. The allowed range of A_{LT}^p was estimated from COMPASS data [29], which resulted in a systematic uncertainty in A_{LT}^n of less than 30% of the statistical uncertainty. Target single-spin-dependent FSI effects on the DSA were canceled by the frequent target spin flips, resulting in negligible uncertainty in the extracted A_{LT}.

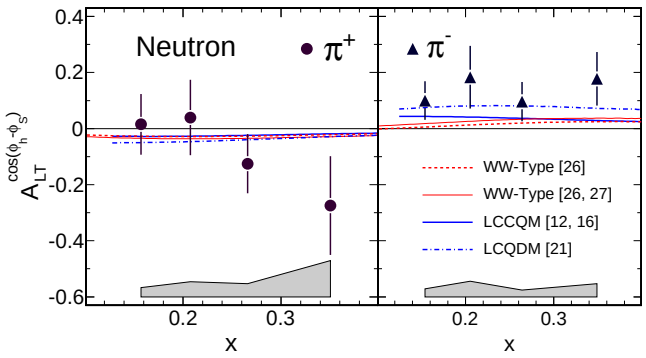

Figure 2. Neutron $A_{LT}^{\cos(\phi_h-\phi_S)}$ azimuthal asymmetry for positive (left) and negative (right) charged pions vs x.

The results are shown in Fig. 2 and are compared to several model calculations, including WW-type approximations with parametrizations from Ref. [26] and Ref. [26, 27], a light-cone constituent quark model (LCCQM) [12, 16] and a light-cone quark-diquark model (LCQDM) evaluated using approach two in Ref. [21]. While the extracted $A_{LT}^n\left(\pi^+\right)$ is consistent with zero within the uncertainties, $A_{LT}^n\left(\pi^-\right)$ is consistent in sign with these model predictions but favors a larger magnitude. Sizable asymmetries could be expected for future experiments, including corresponding SIDIS asymmetries on a proton target and the double-polarized asymmetry in Drell-Yan dilepton production. While the π^+ and π^- data are consistent with the interplay between S-P and P-D wave interference terms predicted by the LCCQM and LCQDM models, the magnitude of the measured π^- asymmetry suggests a larger total contribution from such terms than that found in the LCCQM. The larger magnitude of the data compared to the WW-type calculations suggests either a different $P_{h\perp}$ dependence of A_{LT} than assumed in the calculations, a significant role

for subleading-twist effects, or both. The statistical precision and kinematic coverage of the present data cannot distinguish between these scenarios. It is worth noting that the sign of $A_{LT}^{n}(\pi^-)$ is opposite to the sign of the $A_{UL}^{\sin 2\phi_h}$ asymmetry in π^+ production on the proton measured by the CLAS collaboration [40]. This observation is consistent with many models which support that g_{1T}^{u} and $h_{1L}^{\perp u}$ have opposite signs [23].

In conclusion, we have reported the first measurement of the DSA $A_{LT}^{\cos(\phi_h-\phi_S)}$ in SIDIS using a polarized electron beam on a transversely polarized ^{3}He target. The neutron A_{LT} was also extracted for the first time using the effective polarization approximation. Systematic uncertainties were minimized by forming the raw asymmetry between beam helicity states with minimal charge asymmetry due to the fast helicity reversal. A positive asymmetry was observed for $^3\mathrm{He}\,(e,e'\pi^-)\,X$ and $n\,(e,e'\pi^-)\,X$, providing the first experimental indication of a non-zero A_{LT}, which at leading twist leads to a non-zero g_{1T}^{q}. When combined with measurements on proton and deuteron targets, these new data will aid the flavor-decomposition of the g_{1T}^{q} TMDs. This work has laid the foundation for the future high-precision mapping of A_{LT} following the JLab 12 GeV upgrade [47] and at an electron-ion collider [48], which will provide a comprehensive understanding of the g_{1T}^{q} TMD and the subleading-twist effects.

We acknowledge the outstanding support of the JLab Hall A technical staff and Accelerator Division in accomplishing this experiment. This work was supported in part by the U. S. National Science Foundation, and by U.S. DOE contract DE-AC05-06OR23177, under which Jefferson Science Associates, LLC operates the Thomas Jefferson National Accelerator Facility.

* Corresponding author: jinhuang@jlab.org
† Deceased

[1] P. J. Mulders and R. D. Tangerman, Nucl. Phys. **B461**, 197 (1996).
[2] D. Boer and P. J. Mulders, Phys. Rev. **D57**, 5780 (1998).
[3] A. M. Kotzinian and P. J. Mulders, Phys. Rev. **D54**, 1229 (1996).
[4] X.-D. Ji, J.-P. Ma, and F. Yuan, Nucl. Phys. **B652**, 383 (2003).
[5] R. Jaffe and A. Manohar, Nucl. Phys. **B337**, 509 (1990).
[6] V. Barone, F. Bradamante, and A. Martin, Prog. Part. Nucl. Phys. **65**, 267 (2010).
[7] A. Bacchetta *et al.*, JHEP **02**, 093 (2007).
[8] A. Bacchetta *et al.*, Phys. Rev. **D70**, 117504 (2004).
[9] X.-D. Ji, J.-p. Ma, and F. Yuan, Phys. Rev. **D71**, 034005 (2005).
[10] H. Avakian *et al.* (CLAS), Phys. Rev. **D69**, 112004 (2004).
[11] R. Asaturyan *et al.*, arXiv:1103.1649 [nucl-ex].
[12] S. Boffi *et al.*, Phys. Rev. **D79**, 094012 (2009).
[13] D. de Florian *et al.*, Phys. Rev. Lett. **101**, 072001 (2008).
[14] P. Hagler *et al.*, Europhys. Lett. **88**, 61001 (2009).
[15] R. Jakob, P. Mulders, and J. Rodrigues, Nucl. Phys. **A626**, 937 (1997).
[16] B. Pasquini, S. Cazzaniga, and S. Boffi, Phys. Rev. **D78**, 034025 (2008).
[17] A. Kotzinian, arXiv:0806.3804 [hep-ph].
[18] A. Efremov *et al.*, Phys. Rev. **D80**, 014021 (2009).
[19] H. Avakian *et al.*, Phys. Rev. **D81**, 074035 (2010).
[20] A. Bacchetta *et al.*, Eur. Phys. J. **A45**, 373 (2010).
[21] J. Zhu and B.-Q. Ma, Phys. Lett. **B696**, 246 (2011).
[22] A. V. Efremov *et al.*, J. Phys. Conf. Ser. **295**, 012052 (2011).
[23] C. Lorce and B. Pasquini, arXiv:1104.5651 [hep-ph].
[24] B. U. Musch *et al.*, Phys. Rev. **D83**, 094507 (2011).
[25] E. Di Salvo, Mod. Phys. Lett. **A22**, 1787 (2007).
[26] A. Kotzinian, B. Parsamyan, and A. Prokudin, Phys. Rev. **D73**, 114017 (2006).
[27] A. Prokudin, (private communication).
[28] B. Parsamyan (COMPASS), Eur. Phys. J.ST **162**, 89 (2008).
[29] B. Parsamyan, J. Phys. Conf. Ser. **295**, 012046 (2011).
[30] X. Qian *et al.*, arXiv:1106.0363 [nucl-ex] , accepted to publish in Phys. Rev. Lett.
[31] C. Sinclair *et al.*, Phys. Rev. ST Accel. Beams **10**, 023501 (2007).
[32] D. Androic *et al.* (G0), Nucl. Instrum. Meth. **A646**, 59 (2011).
[33] F. R. P. Bissey *et al.*, Phys. Rev. **C65**, 064317 (2002).
[34] E. Babcock *et al.*, Phys. Rev. Lett. **91**, 123003 (2003).
[35] J. Singh *et al.*, AIP Conf. Proc. **1149**, 823 (2009).
[36] A. Abragam, *Principles of Nuclear Magnetism* (Oxford University, New York, 1961).
[37] M. V. Romalis and G. D. Cates, Phys. Rev. A **58**, 3004 (1998).
[38] J. Alcorn *et al.*, Nucl. Instrum. Meth. **A522**, 294 (2004).
[39] A. Raskin and T. Donnelly, Annals Phys. **191**, 78 (1989).
[40] H. Avakian *et al.* (CLAS), Phys. Rev. Lett. **105**, 262002 (2010).
[41] K. Abe *et al.* (E143 Collaboration), Phys. Lett. **B452**, 194 (1999).
[42] I. Akushevich *et al.*, Comput. Phys. Commun. **104**, 201 (1997).
[43] T. Sjostrand, S. Mrenna, and P. Z. Skands, JHEP **0605**, 026 (2006).
[44] A. Airapetian *et al.* (HERMES), Phys. Rev. Lett. **94**, 012002 (2005).
[45] A. Airapetian *et al.* (HERMES), Phys. Lett. **B693**, 11 (2010).
[46] X. Zheng *et al.* (Jefferson Lab Hall A Collaboration), Phys. Rev. Lett. **92**, 012004 (2004).
[47] H. Gao *et al.*, Eur. Phys. J.Plus **126**, 1 (2011).
[48] M. Anselmino *et al.*, Eur. Phys. J. **A47**, 35 (2011).

x	Q^2 GeV^2	y	z	$P_{h\perp}$ GeV	^{3}He $A_{LT}^{\cos(\phi_h-\phi_S)}$ π^+	^{3}He $A_{LT}^{\cos(\phi_h-\phi_S)}$ π^-	neutron $A_{LT}^{\cos(\phi_h-\phi_S)}$ π^+	neutron $A_{LT}^{\cos(\phi_h-\phi_S)}$ π^-
0.156	1.38	0.81	0.50	0.43	$+0.003 \pm 0.020 \pm 0.004$	$+0.030 \pm 0.020 \pm 0.008$	$+0.02 \pm 0.11 \pm 0.03$	$+0.10 \pm 0.07 \pm 0.03$
0.206	1.76	0.78	0.52	0.38	$+0.005 \pm 0.016 \pm 0.004$	$+0.032 \pm 0.019 \pm 0.007$	$+0.04 \pm 0.13 \pm 0.05$	$+0.18 \pm 0.11 \pm 0.06$
0.265	2.16	0.75	0.54	0.32	$-0.019 \pm 0.015 \pm 0.003$	$+0.024 \pm 0.017 \pm 0.004$	$-0.13 \pm 0.11 \pm 0.05$	$+0.10 \pm 0.07 \pm 0.02$
0.349	2.68	0.70	0.58	0.24	$-0.025 \pm 0.015 \pm 0.005$	$+0.034 \pm 0.017 \pm 0.006$	$-0.27 \pm 0.18 \pm 0.13$	$+0.18 \pm 0.10 \pm 0.05$

Table I. Central kinematics and asymmetry results. The format for ^{3}He and neutron $A_{LT}^{\cos(\phi_h-\phi_S)}$ asymmetries follows "central value" ± "statistical uncertainty" ± "systematic uncertainty" .